Supplemental material for "Self-propulsion of pure water droplets by spontaneous Marangoni stress driven motion"

Ziane Izri,[1] Marjolein N. van der Linden,[1] Sébastien Michelin,[2] and Olivier Dauchot[1]

[1] EC2M, UMR Gulliver 7083 CNRS, ESPCI ParisTech,
PSL Research University, 10 rue Vauquelin, 75005 Paris, France
[2] LadHyX – Département de Mécanique, Ecole Polytechnique – CNRS, 91128 Palaiseau, France

In the main manuscript, we showed that the linear stability analysis for an isotropic active droplet is essentially identical to that of an active autophoretic particle provided the phoretic mobility M is replaced by

$$M' = \frac{aK + 3\eta_i M}{2\eta_o + 3\eta_i},$$ (1)

where η_i and η_o are the fluid viscosities inside and outside the droplet, respectively, and K defines the linear relationship between the local surface tension gradient $\nabla_\parallel \gamma$ and the local solute concentration gradient. In this supplementary material, we provide the full details on the coupled Stokes and advection-diffusion problem, and show that although qualitatively similar the nonlinear dynamics and saturation velocity differ between the droplet and solid particle cases.

The droplet is assumed to remain spherical at all times (i.e. the capillary number $\text{Ca} = \eta U^*/\gamma$ is small where U^* is the characteristic droplet velocity). The normal unit vector at the surface is $\mathbf{n} = \mathbf{e}_r$, and $\nabla_\parallel = (\mathbf{I} - \mathbf{nn}) \cdot \nabla$ is the tangential gradient operator. We focus on an axisymmetric problem such that all fields depend only on r and $\mu = \cos\theta$, with θ the polar angle in spherical polar coordinates.

The solute is released from the droplet's surface ($r = a$) at a constant flux A, such that the boundary condition for the solute dynamics on the droplet's surface can be written as

$$D\mathbf{n} \cdot \nabla C|_{(r=a)} = -A.$$ (2)

The solute is then advected by the outer flow and diffuses with diffusivity D:

$$\frac{\partial C}{\partial t} + \mathbf{u}^o \cdot \nabla C = D\nabla^2 C.$$ (3)

A uniform concentration C_∞ is assumed in the far-field (e.g. zero). Flows inside and outside the droplet satisfy Stokes equations (i.e. the Reynolds number $\text{Re} = U^*a/\eta$ is small)

$$\eta_i \nabla^2 \mathbf{u}^{o,i} = \nabla p^{o,i}, \quad \nabla \cdot \mathbf{u}^{o,i} = 0,$$ (4)

where superscripts ^{i} and ^{o} on hydrodynamic fields refer to the inner ($r < a$) and outer ($r > a$) flows, respectively. Considering a reference frame attached to the droplet's center, the boundary condition at infinity is obtained as

$$\mathbf{u}^o(r \to \infty) \sim -\mathbf{U},$$ (5)

with $\mathbf{U}$ the droplet's velocity (there is no rotation here due to the axisymmetry). At the droplet's surface, inhomogeneities in the local solute concentration lead to tangential velocity and stress jumps:

$$\mathbf{u}_j = (\mathbf{u}^o - \mathbf{u}^i)_{(r=a)} = M \nabla_\parallel C|_{(r=a)},$$ (6)

$$\boldsymbol{\tau}_j = [(\mathbf{I} - \mathbf{nn}) \cdot (\boldsymbol{\sigma}^o - \boldsymbol{\sigma}^i) \cdot \mathbf{n}]_{(r=a)} = \nabla_\parallel \gamma|_{(r=a)} = -K\nabla_\parallel C|_{(r=a)}.$$ (7)

Finally, inertia is negligible and assuming there is no external body force (e.g. buoyancy), the droplet must remain force-free at all times

$$\int_{(r=a)} \boldsymbol{\sigma}^o \cdot \mathbf{n} dS = 0.$$ (8)

Equations (2)–(8) form a closed and well-posed set of equations for the solute concentration $C(r, \mu)$ outside the droplet and the flow fields $\mathbf{u}^i$ and $\mathbf{u}^o$ inside and outside the droplet. Because of the spherical geometry, the hydrodynamic problem, Eqs. (4)–(5) and (8) can be solved formally and analytically as follows, using the squirmer model [1, 5]. The flow is axisymmetric, and can therefore be computed from the streamfunction $\psi(r, \mu, t)$, as

$$\mathbf{u} = -\frac{1}{r^2}\frac{\partial \psi}{\partial \mu}\mathbf{e}_r - \frac{1}{r\sqrt{1-\mu^2}}\frac{\partial \psi}{\partial r}\mathbf{e}_\theta.$$ (9)

The streamfunction $\psi(r, \mu, t)$ is decomposed azimuthally inside and outside the droplet,

$$\psi^{o,i}(r, \mu, t) = \sum_{n=1}^{\infty} \frac{2n+1}{n(n+1)} \alpha_n^{o,i}(t) \psi_n^{o,i}(r)(1 - \mu^2) L_n'(\mu), \tag{10}$$

with $L_n(\mu)$ the Legendre polynomial of order n. $\alpha_n^o(t)$ and $\alpha_n^i(t)$ are the outer and inner squirming mode intensities and may differ when the velocity jump $\mathbf{u}_j$ is non zero. Inside and outside the droplet, the radial part of the streamfunction must be of the form [2, 4]

$$\psi_n^{o,i}(r) = E_n^{o,i} r^{n+3} + F_n^{o,i} r^{n+1} + G_n^{o,i} r^{2-n} + H_n^{o,i} r^{-n}, \tag{11}$$

where $E_n^{o,i}, F_n^{o,i}, G_n^{o,i}$ and $H_n^{o,i}$ are constants to be determined using regularity and boundary conditions in each domain. Using the force-free condition, Eq. (8) ($G_1^o = 0$), the impermeability condition ($\psi_n^o(a) = 0$) and the far-field behavior of the flow, Eq. (5), the outer radial modes $\psi_n^0(r)$ are obtained as [4, 5]

$$\psi_1^o(r) = \frac{a^3}{3r} - \frac{r^2}{3}, \qquad \psi_n^o(r) = \frac{1}{2}\left(\frac{a^{n+2}}{r^n} - \frac{a^n}{r^{n-2}}\right) \quad \text{for } n \geq 2. \tag{12}$$

In particular, $\alpha_1^o(t) = U(t)$ is the swimming velocity of the droplet. The second mode, $n = 2$, corresponds to the intensity of the slowest-decaying singularity created by the self-propelled droplet, namely that of a symmetric force dipole or stresslet. Enforcing the regularity of the flow field inside the droplet ($G_n^i = H_n^i = 0$) and the impermeability condition ($\psi_n^i(a) = 0$), the inner radial modes $\psi_n^i(r)$ are obtained as

$$\psi_n^i(r) = \frac{1}{2}\left(\frac{r^{n+1}}{a^{n-1}} - \frac{r^{n+3}}{a^{n+1}}\right). \tag{13}$$

Finally, decomposing the solute concentration azimuthally, $C(r, \mu, t) = \sum C_p(r, t) L_p(\mu)$, the different modes $C_p(r, t)$ satisfy the following system of partial differential equations in the outer fluid:

$$\frac{\partial C_p}{\partial t} + \frac{1}{r^2} \sum_{m=0}^{\infty} \sum_{n=1}^{\infty} \alpha_n^o(t)\left(A_{mnp}\frac{\partial C_m}{\partial r}\psi_n^o + B_{mnp}C_m\frac{\mathrm{d}\psi_n^o}{\mathrm{d}r}\right) = \frac{D}{r^2}\left[\frac{\partial}{\partial r}\left(r^2\frac{\partial C_p}{\partial r}\right) - p(p+1)C_p\right], \tag{14}$$

with boundary conditions

$$D\frac{\partial C_p}{\partial r}(r = a) = -A\delta_{p0}, \qquad C_p(r \rightarrow \infty) \rightarrow C_\infty \delta_{p0}. \tag{15}$$

The tensors A_{mnp} and B_{mnp} are defined as

$$A_{mnp} = \frac{(2p+1)(2n+1)}{2}\int_{-1}^{1} L_m(\mu)L_n(\mu)L_p(\mu)\mathrm{d}mu, \quad B_{mnp} = \frac{(2p+1)(2n+1)}{2n(n+1)}\int_{-1}^{1}(1 - \mu^2)L_m'(\mu)L_n'(\mu)L_p(\mu)\mathrm{d}\mu \tag{16}$$

The solute is released from the droplet's surface into the outer fluid only, where it is advected and diffuses. Hence, its dynamics is not impacted by the flow inside the droplet, and to solve this advection-diffusion problem for $C_p(r, t)$, one only needs to know the outside flow (i.e. $\alpha_n^o(t)$).

Using Eqs. (9) and (10), the velocity jump condition, Eq. (6), can now be written in terms of $\alpha_n^{o,i}$:

$$\alpha_n^o - \alpha_n^i = -\frac{n(n+1)}{2n+1}\frac{M}{a}C_n(a, t). \tag{17}$$

The stress jump condition, Eq. (7), writes

$$\left(\sigma_{r\theta}^o - \sigma_{r\theta}^i\right)(r = a) = \frac{K\sqrt{1 - \mu^2}}{a}\frac{\partial C}{\partial \mu}(r = a) \tag{18}$$

with the stress tensor component $\sigma_{r\theta}$ obtained inside and outside the droplet using

$$\sigma_{r\theta}^{o,i} = \eta_{o,i}\left[r\frac{\partial}{\partial r}\left(\frac{u_\theta^{o,i}}{r}\right) - \frac{\sqrt{1 - \mu^2}}{r}\frac{\partial u_r^{o,i}}{\partial \mu}\right] = -\eta_{o,i}\sqrt{1 - \mu^2}\sum_{n=1}^{\infty}\frac{2n+1}{n(n+1)}\alpha_n^{o,i}(t)L_n'(\mu)\left[r\frac{\mathrm{d}}{\mathrm{d}r}\left(\frac{1}{r^2}\frac{\mathrm{d}\psi_n^{o,i}}{\mathrm{d}r}\right) + \frac{n(n+1)}{r^3}\psi_n^{o,i}\right].$$
$$\tag{19}$$

Applying the stress jump condition on $r = a$, we obtain

$$3\eta_o \alpha_1^o + \frac{9\eta_i}{2}\alpha_1^i = -KC_1(a,t), \qquad \eta_o \alpha_n^o + \eta_i \alpha_n^i = -\frac{n(n+1)}{(2n+1)^2}KC_n(a,t) \text{ for } n \geq 2. \tag{20}$$

Equations (17) and (20) form a linear system for α_n^o and α_n^i that can be inverted to obtain $\alpha_n^o(t)$ as a function of $C_n(a,t)$, and the entire flow field outside the droplet (the flow inside the droplet can be recovered similarly):

$$\alpha_1^o(t) = -\frac{2}{3}\left(\frac{aK + 3\eta_i M}{2\eta_o + 3\eta_i}\right)\frac{C_1(a,t)}{a}, \tag{21}$$

$$\alpha_n^o(t) = -\frac{n(n+1)}{(2n+1)^2}\left(\frac{aK + M\eta_i(2n+1)}{\eta_o + \eta_i}\right)\frac{C_n(a,t)}{a}, \tag{22}$$

As we pointed out earlier, the solute dynamics only requires the knowledge of the outer flow or $\alpha_n^o(t)$, as for the problem of a rigid phoretic particle. In both cases, $\alpha_n^o(t)$ is proportional to $C_n(a,t)$, Eqs. (21)–(22), but the coefficient of proportionality (and its variation with n) differs between the two cases.

Repeating the analysis of [8] in the case of a droplet, we consider the stability of the trivial isotropic and steady solution to the coupled Stokes and advection-diffusion problems above, $\bar{C}(r) = Aa^2/Dr$, which leads to no tangential gradients and therefore no flow ($\bar{\alpha}_n^{o,i} = 0$). Decomposing the perturbation $C'(r,\mu,t)$ azimuthally, the equation for the first azimuthal mode $C_1'(r,t)$ is obtained, at leading order in the perturbation, from Eq. (14) with $p = 1$ as

$$\frac{\partial C_1}{\partial t} - \frac{D}{r^2}\left[\frac{\partial}{\partial r}\left(r^2\frac{\partial C_1}{\partial r}\right) - 2C_1\right] = -\frac{3\alpha_1^o(t)}{r^2}\frac{\mathrm{d}\bar{C}}{\mathrm{d}r}\psi_1^o = \frac{\alpha_1^o(t)Aa^2}{Dr^2}\left(\frac{a^3}{r^3} - 1\right) \tag{23}$$

and one can observe that $\alpha_1^o(t)$ is the only squirming mode influencing the linear instability leading to self-propulsion. Hence, Eqs. (21) and (23) are strictly identical to the case of a rigid phoretic particle (Eqs. (10) and (11) in [8]) provided the substitution Eq. (1) is performed. The linear stability result of [8] for the swimming mode is therefore directly applicable to the droplet case and spontaneous self-propulsion of isotropic spherical droplets is predicted provided $AM' > 0$ and $\text{Pe} = |AM'|a/D^2 \geq 4$. To investigate the nonlinear saturated dynamics beyond the instability threshold, all modes must be considered and the result is now modified from the rigid particle case.

In terms of swimming velocity, the rigid particle limit is recovered when $\eta_i M/aK \gg 1$ or equivalently given the scalings of M and K in the main text when $\eta_i/\eta_o \gg a/\lambda$ which is essentially only achieved for a rigid particle, since $\lambda \ll a$. For a droplet, the Marangoni terms dominate systematically, except for very high order modes as suggested by Eq. (22). From a numerical point of view however, in the Marangoni limit ($\eta_i/\eta_o \to \infty$), the convergence of the result with the number of squirming modes is faster than for the phoretic case ($\alpha_n^o = O(C_n)$ in the Marangoni limit rather than $\alpha_n^o = O(nC_n)$ in the phoretic limit). High-order modes therefore only have a negligible contribution to the flow field, except if $\text{Pe} \gg 1$ (in that case the flow field and the solute distribution become strongly polarized azimuthally [6, 7]).

Equations (14), (15), (21) and (22) can be solved numerically using the numerical methods described in [6, 7] and the result is shown in Figure 1 in the pure Marangoni limit and with $\eta_i/\eta_o = 1/36$. The evolution of the velocity with Pe is qualitatively similar to that obtained by [8] for a rigid phoretic particle, albeit slightly larger. Also, as for rigid phoretic particles, self-propelling droplets are always pushers ($\Sigma < 0$), meaning that their far-field signature is similar to the flow field generated by flagellated bacteria [3].

[1] J. R. Blake. A spherical envelope approach to ciliary propulsion. *J. Fluid Mech.*, 46:199–208, 1971.
[2] J. Happel and H. Brenner. *Low Reynolds Number Hydrodynamics*. Prentice Hall, Englewood Cliffs, NJ, 1965.
[3] E. Lauga and T. R. Powers. The hydrodynamics of swimming micro-organisms. *Rep. Prog. Phys.*, 72:096601, 2009.
[4] L. G. Leal. *Advanced Transport Phenomena, Fluid Mechanics and Convective Transport Processes*. Cambridge University Press, New York, 2007.
[5] S. Michelin and E. Lauga. Optimal feeding is optimal swimming for all Péclet numbers. *Phys. Fluids*, 23(10):101901, 2011.
[6] S. Michelin and E. Lauga. Unsteady feeding and optimal strokes of model ciliates. *J. Fluid Mech.*, 715:1–31, 2013.
[7] S. Michelin and E. Lauga. Phoretic self-propulsion at finite péclet numbers. *J. Fluid Mech.*, 747:572–604, 2014.
[8] S. Michelin, E. Lauga, and D. Bartolo. Spontaneous autophoretic motion of isotropic particles. *Phys. Fluids*, 25:061701, 2013.
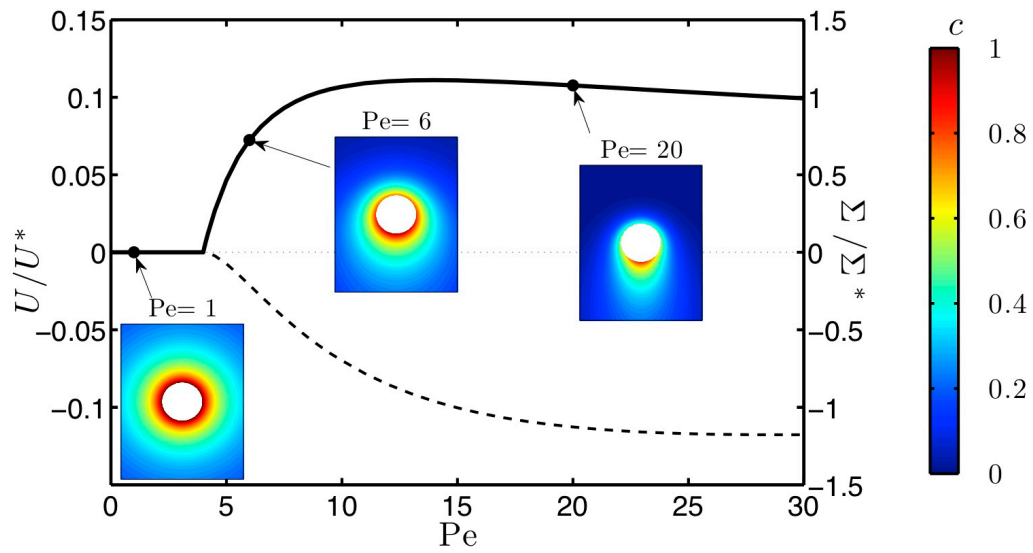
FIG. 1: Evolution with Pe $= U^*a/D$ of the non-dimensional droplet velocity U/U^* with $U^* = |AM'|/D$ and the non-dimensional stresslet $10\pi\alpha_2^o$. The non-dimensional relative concentration $c = (C - C_\infty)/(Aa/D)$ is also shown for selected Pe, showing the symmetry breaking in the solute distribution associated with self-propulsion, despite the isotropy of the solute flux at the droplet boundary.